Desalination and Water Treatment
www.deswater.com

doi: 10.5004/dwt.2017.20994

80 (2017) 223–233
June

Highly efficient capture of Cu(II) by magnetic graphene oxide from aqueous solution: influences of pH, ionic strength, temperature, soil humic acid and fulvic acid

Chengan Jin[a], Wensheng Linghu[a,*], Lianyang Zhang[b], Jun Hu[c], Yang Jin[a,b], Di Xu[d], Guodong Sheng[a,e,*]

[a]*College of Chemistry and Chemical Engineering, Shaoxing University, Zhejiang 312000, China, Fax: +86 575 8834 1521; emails: wslinghu@usx.edu.cn (W. Linghu), gdsheng@usx.edu.cn (G. Sheng), 409331859@qq.com (C. Jin), jyk@usx.edu.cn (Y. Jin)*
[b]*Key Laboratory of Clean Dyeing and Finishing Technology of Zhejiang Province, Shaoxing University, Zhejiang 312000, China, email: 1175308147@qq.com*
[c]*School of Electronic Engineering, Dongguan University of Technology, Guangdong 523808, China, email: hu_ipp@126.com*
[d]*State Key Laboratory of Lake Science and Environment, Nanjing Institute of Geography and Limnology, Chinese Academy of Sciences, Nanjing 210008, China, email: dxu@niglas.ac.cn*
[e]*NAAM Research Group, Faculty of Science, King Abdulaziz University, Jeddah 21589, Saudi Arabia*

Received 11 January 2017; Accepted 29 May 2017

ABSTRACT

In this study, the capture of Cu(II) from aqueous solution by magnetic graphene oxide (MGO) via an adsorption process in the absence and presence of humic acid (HA) or fulvic acid (FA) was investigated by using a batch technique. The effects of contact time, pH, ionic strength, coexisting cations or anions and temperature were studied. The results indicated that the Cu(II) sorption is strongly dependent on pH but independent on ionic strength. A positive effect of HA/FA on Cu(II) adsorption was found at pH < 7.5, whereas a negative effect was observed at pH > 7.5. The adsorption isotherms can be described by the Langmuir model as well as the Freundlich model in the absence and presence of HA/FA. Adsorption isotherms of Cu(II) at higher initial HA/FA concentrations are higher than those at lower FA/HA concentrations. The thermodynamic parameters were calculated from the temperature isotherms, and the results suggested that the sorption was a spontaneous and endothermic process. Results of this work suggest that MGO may be a promising adsorbent for the treatment of heavy metal ions from aqueous solutions.

Keywords: Magnetic graphene oxide; Cu(II); Humic acid; Fulvic acid; Adsorption

1. Introduction

Due to the rapid development of agriculture and industry, heavy metal contamination has become a serious environmental problem, which is a threat to human health and ecological systems [1–3]. Among these metal ions, Cu(II) is one of the most important pollutants affirmed as by US EPA, since excessive Cu(II) consumption can cause hazardous effect on public health [4,5]. The source of Cu(II)-contaminated wastewater is quite widespread, including copper smelting, electroplating and other industrial activities [4,5]. Therefore, treating Cu(II) wastewater is very necessary and has attracted considerable interest. So far, various techniques have been developed for treating Cu(II)-contaminated wastewater, such as adsorption [6–9], membrane filtration [10], ion-exchange [11], biological treatment [12] and chemical precipitation [13]. Among them, adsorption with the advantages of simple operation, high efficiency and low-cost, is considered as an attractive choice for treating wastewater [14,15]. Thus, a variety of absorbents were used to treat Cu(II) contaminated wastewater, such as electric furnace slag [16], grafted silica [17], carbon nanotubes [18], loofah fibers [9],

---

* Corresponding author.

bentonite [19], etc. Although these adsorbents have good adsorption about copper, the difficult separation and lack of stability make them restricted in the practical application. In order to improve these problems, it is crucial to find an absorbent with good stability and the advantage of simple post-processing.

Graphene oxide (GO), which has large surface area and various oxygen-containing functional groups, such as (–OH), carboxyl (–COOH) and epoxy (–C–O–C–), is considered as an ideal adsorbent to eliminate organic and inorganic pollutants in the water treatment [20–22]. So far, multifarious graphene-based environment functional materials have been synthesized and been widely applied in treating various wastewater within a short time [21–30]. Especially, in recent years, the preparation and application of magnetic graphene oxide (MGO) and its derivative materials have received widespread attention, which mainly due to their outstanding adsorb ability to contaminants and simple separation [8,24,26,29–34]. For example, Chandra et al. [31] synthesized MGO with a magnetite particle size of ~10 nm, and showed nearly complete arsenic removal within 1 ppb. Yu et al. [32] reported the adsorption of arsenate and arsenite on MGO with adsorption capacities of 54.18 and 26.76 mg/g, respectively. Wang et al. [33] successfully synthesized a novel composite, that is, MGO modified with β-cyclodextrin and ethylenediamine (CD-E-MGO), and used it for dealing with Cr(VI) wastewater. In addition, MGO also plays a significant role in disposing organic pollutants. Yao et al. [24] investigated the adsorption properties of MGO toward methylene blue (MB) and congo red in aqueous solution. Zhang et al. [34] developed a polyacrylic acid (PAA) functionalized magnetic graphene oxide nanocomposite (PAA/MGO) for the removal of MB from wastewater. However, lots of studies have been focused on the application of MGO in treating independent inorganic or organic pollutants. There is few studies consider the effect of organic pollutant on the removal of heavy metal ions and vice versa [8], while it should be aware of the fact that heavy metal ions and organic pollutant may present simultaneously at pollution systems [35]. Therefore, it is of great interest to study the removal and interaction mechanism of heavy metal ions by MGO in the presence of organic pollutant and vice versa.

In this work, MGO is used as adsorbent to remove Cu(II) from aqueous solutions in the absence and presence of humic acid (HA) or fulvic acid (FA), which is widely present in the environment. The basic objectives of this research are: (1) to investigate the effect of contact time, pH, initial Cu(II) concentration, ionic strength, foreign ions and temperature on Cu(II) adsorption; (2) to conduct Cu(II) adsorption as affected by the different concentrations of HA or FA; (3) to study Cu(II) adsorption from both thermodynamic and kinetic viewpoints and (4) to discuss the possible mechanisms of Cu(II) adsorption on MGO.

2. Experimental process

2.1. Materials

Graphite powder (70 um) was purchased from Qingdao Graphite Company (China). HA and FA were given by the Institute of Plasma Physics, Chinese Academy of Sciences, which were obtained from Hua-jia county's soil (Gansu, China), and the detailed characterizations were in their previous work [36]. All other chemicals were analytical grade and used without further purified. Milli-Q water was used in the whole experiment.

2.2. Synthesis of GO and MGO

GO and MGO were synthesized on the basis of previous work in detail [26,37,38]. GO was synthesized from graphite power according to the modified Hummers method [37,38]. MGO was synthesized by the chemical coprecipitation of $FeCl_2·4H_2O$ (0.52 g) and $FeCl_3·6H_2O$ (2.79 g) in an ammonia solution in the presence of GO (0.3 g) under N_2 conditions [26]. The mixed solution of Fe^{2+}/Fe^{3+} (1:2) was added slowly to the GO suspension, and then $NH_3·H_2O$ was added swiftly to precipitate Fe^{2+}/Fe^{3+} ions for generating Fe_3O_4 at pH 10–11. The mixed solution temperature was raised to ~85°C, and kept stirring for ~1 h, then cooled down to room temperature. After that, the MGO separated from the dark black colored solution by filtration, washed with Milli-Q water, and dried at ~70°C. The GO and MGO composites were obtained and characterized by scanning electron microscope (SEM), and the results are shown in Fig. 1. It is distinct that the Fe_3O_4 nanoparticles were successfully

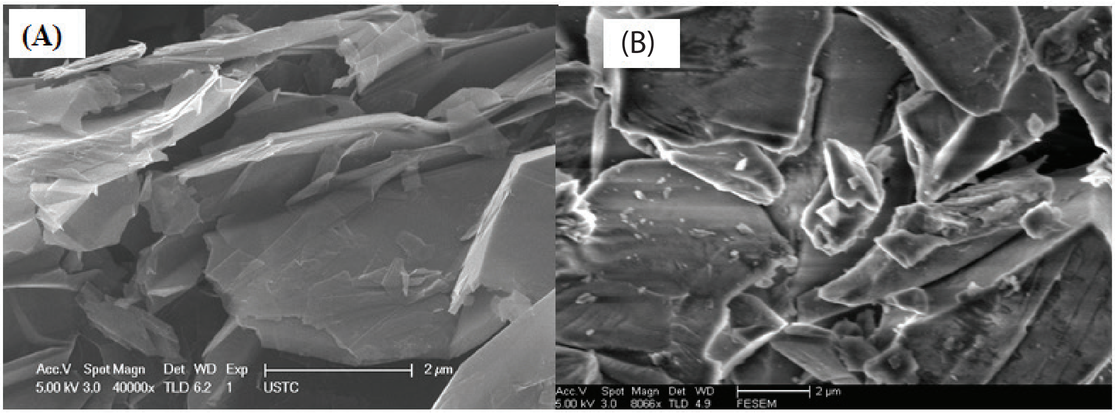

Fig. 1. SEM images of GO (A) and MGO (B) composites.

loaded on GO surfaces and the sheets of GO was crumpled, which can be compared with Figs. 1(A) and (B), respectively.

2.3. Batch sorption experiments

The batch sorption experiments were carried out as follows: first, the preparation of 4 g/L MGO stock suspensions (0.1 g of MGO dispersed into a 25 mL of Milli-Q water by ultrasonic technique). Second, for the Cu(II) adsorption: (1) MGO homogeneous suspension was added to polyethylene (PE) tube by using an injector; (2) After that, the stock solution of $NaNO_3$, $Cu(NO_3)_2$ and water were added to PE tube to get desired concentrations of various components. And pH was adjusted by adding inappreciable volumes of 0.01 mol/L of HNO_3 or NaOH. Subsequently, the PE tube was shaken for 180 min to reach the adsorption equilibrium, and then the magnetic separation method was used for separating the solid and liquid. Cu(II) concentration was determined by atomic absorption spectroscopy. The sorption percentage and sorption capacity of Cu(II) were calculated by Eqs. (1) and (2):

$$\text{Sorption\%} = \frac{C_0 - C_e}{C_0} \times 100\% \tag{1}$$

$$q_e = \frac{C_0 - C_e}{C_0} \times \frac{V}{m} \tag{2}$$

where C_0 (mg/L) represents the initial Cu(II) concentration, C_e (mg/L) is the Cu(II) concentration in the supernatant after magnetic separation, q_e (mg/g) is the adsorbed amount of Cu(II) on MGO at equilibrium time, m (g) is the mass of the MGO and V (L) is the volume of the solution.

3. Results and discussion

3.1. Influence of contact time and kinetics study

The effect of contact time on the removal of Cu(II) from aqueous solution by MGO with different initial Cu(II) concentration is shown in Fig. 2(A). The sorption of Cu(II) on MGO increases quickly during the first 120 min, then remains unchanged with increasing contact time. In order to further study the Cu(II) sorption rate, the pseudo-second-order (Eq. (3)) and pseudo-first-order (Eq. (4)) rate equations were used to fit the adsorption data, the linear form of which are as follows [39]:

$$\frac{t}{q_t} = \frac{1}{2Kq_e^2} + \frac{1}{q_e}t \tag{3}$$

$$\ln(q_e - q_t) = \ln q_e - kt \tag{4}$$

where q_t (mg/g) is the amount of Cu(II) adsorbed on MGO at time t (min), and q_e (mg/g) is Cu(II) adsorption amount at equilibrium time. K (g/(mg·min)) and k (min^{-1}) are the pseudo-second-order and pseudo-first-order rate parameters, respectively. Judging from Figs. 2(B) and (C), we can see that the kinetic adsorption of Cu(II) on MGO can be well described by the pseudo-second-order than the pseudo-first-order rate equation.

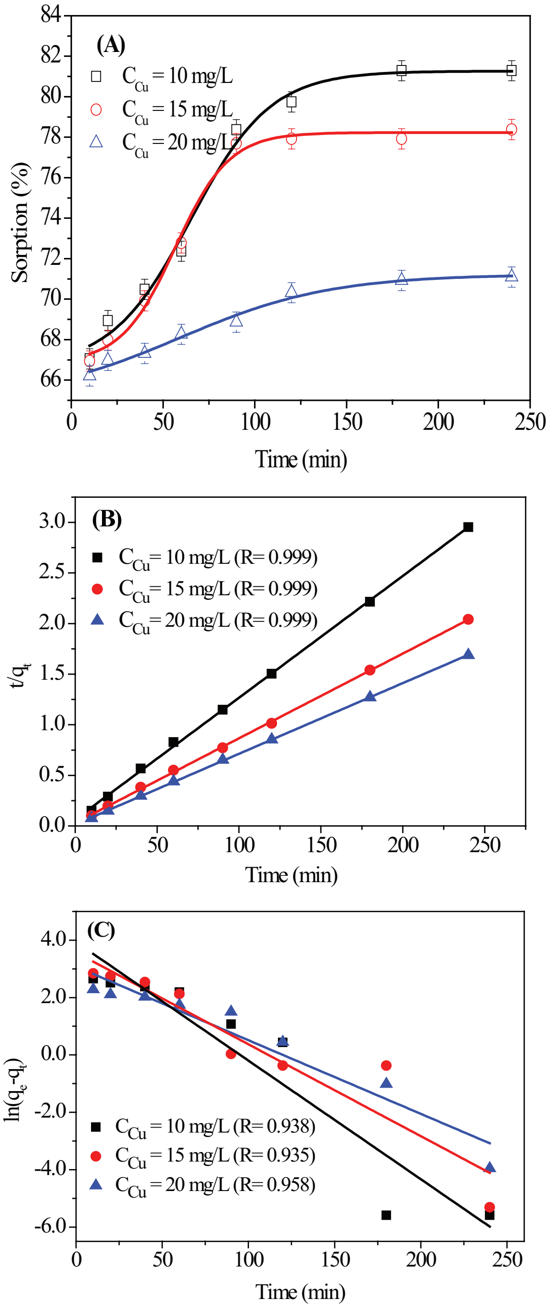

Fig. 2. (A) Influence of contact time on the adsorption of Cu(II) onto MGO, (B) plots of pseudo-second-order kinetic model and (C) plots of pseudo-first-order kinetic model, initial pH = 5.0 ± 0.2, m/V = 0.1 g/L, I = 0.01 mol/L $NaClO_4$, T = 293 K.

3.2. Influence of initial solution pH

Fig. 3(A) shows that the initial pH of solution plays a significant role in Cu(II) removal by MGO. The adsorption of Cu(II) on MGO increases gradually at pH 3.0–4.5, then increases promptly at pH 4.5–7.5, finally maintains a high level (~100%) at pH > 7.5. Similar results were also reported for Cu(II) sorption on other adsorbents like polyacrylamide grafted bentonite (Bent-PAAM) and multiwalled carbon nanotubes (MWCNTs) [40,41]. According to

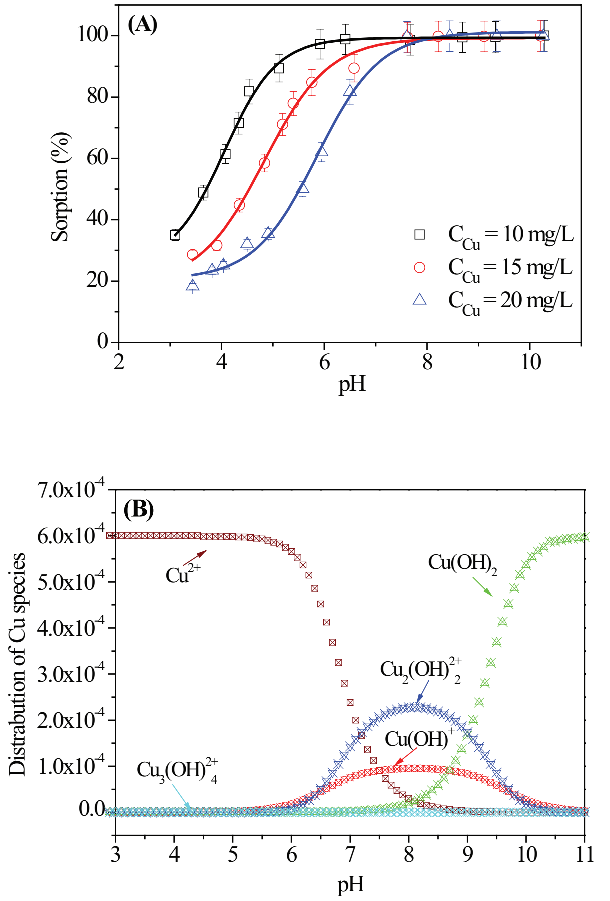

Fig. 3. (A) Influence of pH on Cu(II) adsorption onto MGO, $m/V = 0.1$ g/L, $I = 0.01$ mol/L $NaClO_4$, $T = 293$ K. (B) Distribution of Cu(II) species as a function of pH.

the Cu(II) hydrolysis constants ($\log K_1 = –7.5$, $\log K_2 = –17.3$, $\log K_3 = –27.3$, $\log K_4 = –10.36$ and $\log K_5 = –39.6$) [42], the relative species of Cu(II) as a function of pH is shown in Fig. 3(B). It is distinct that Cu^{2+} mainly exists in the solution at pH < 7.5, and $Cu_2(OH)_2^{2+}$, $Cu(OH)^+$ and $Cu(OH)_2^0$ are major compositions at pH 7.5–11.0. It was reported that the pH_{zpc} of GMO was ~4.5 [8]. So, at pH < pH_{zpc}, the protonation reaction may take place on the MGO surface, and it brings about Cu(II) low sorption because of the electrostatic repulsion between positively charged MGO and Cu^{2+}. At pH > pH_{zpc}, the GMO surfaces become negatively charged due to deprotonation reaction, thus the Cu(II) species like Cu^{2+}, $Cu_2(OH)_2^{2+}$ and $Cu(OH)^+$ can be easily adsorbed by MGO.

3.3. Influence of ionic strength

Fig. 4(A) shows that the effect of ionic strength on Cu(II) sorption as a function of pH in 0.001, 0.01 and 0.1 mol/L $NaClO_4$ solutions, respectively. It is obvious that ionic strength has little impact on the removal of Cu(II) on MGO at pH 3.0–11.0. And similar results were reported in the literature [8,41]. The ionic strength can affect the thickness and interface potential of the double layer, and further influence the binding of adsorbed species [43]. The ionic strength effect on outer-sphere surface complexation is remarkable; however, inner-sphere surface complexation is not influenced by the ionic strength [41,44]. Consequently, adsorption of Cu(II) may be owe to take shape about inner-sphere complexes on the surfaces of MGO. Hayes and Leckie [45] proposed that sorption reaction can be deduced in regard with the impact of the background electrolyte on the sorption reaction. As a rule, when the sorption reaction is observably influenced by the background electrolyte, it can be regarded as β-plane sorption; if not, *o*-plane sorption is likely to occur. Thus, judging from the results of this work, copper ion may take part in *o*-plane sorption reaction because the background electrolyte (Na^+ and ClO_4^-) has almost no effect on the sorption reaction. On the whole, the pH-dependent and ionic strength-independent of Cu(II) sorption on MGO manifest that the main mechanism of Cu(II) sorption is inner-sphere surface complexation.

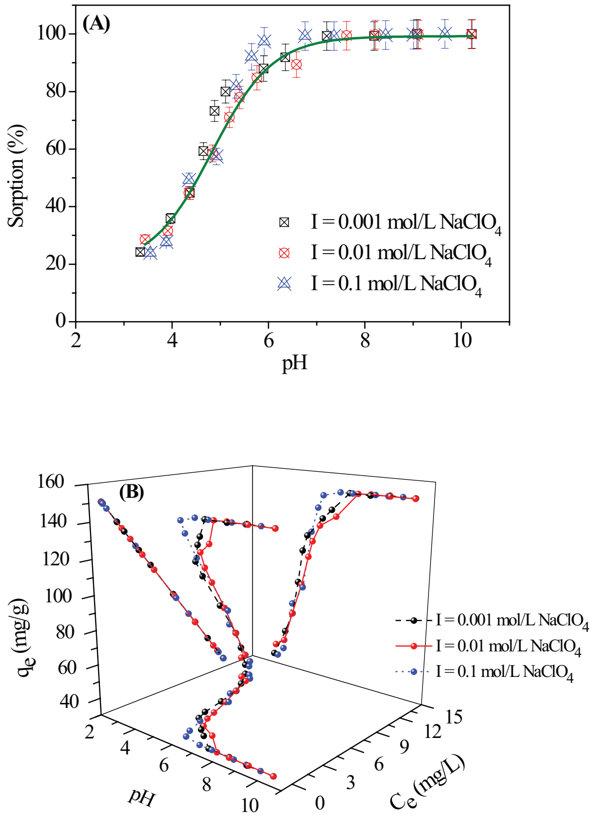

Fig. 4. (A) Influence of ionic strength Cu(II) adsorption onto MGO, and (B) 3D plots of q_e, C_e and pH, $C_{Cu} = 15$ mg/L, $m/V = 0.1$ g/L, $T = 293$ K.

In order to analyze the relationship and variation of pH, C_e and q_e, 3D are obtained by the experimental data and shown in Fig. 4(A). From the plane of pH–q_e, the variation trends are approximately similar to those of pH–sorption (Fig. 4(A)). The projection on the pH–C_e plane (Fig. 4(B)) is merely the inverted image of the projection on the pH–q_e plane. As showed in the C_e–q_e plane, one can see that all the experimental data display in a straight line. It is clear that the initial Cu(II) concentration is uniform in each experimental point. The relationship of C_e–q_e can be described by [46]:

$$VC_o = mq_e + VC_e \quad (5)$$

Eq. (5) can be rearranged and expressed in the linear form:

$$q_e = -\frac{V}{m}C_e + \frac{V}{m}C_0 \tag{6}$$

The straight line of C_e–q_e with slope ($-V/m$) and intercept (C_0V/m) is shown clearly in Eq. (6). The values of slope ($-V/m = -10$) and intercept ($C_0V/m = 150$) are calculated from C_e–q_e line, which are in agreement with the values of $m/V = 0.1$ g/L and $C_0V/m = 150$ mg/g, respectively.

3.4. Influence of cations and anions

To investigate the impact of foreign cations and anions on the removal of Cu(II), the Cu(II) sorption on MGO as a function of pH values that was explored in the presence of 0.01 mol/L $LiClO_4$, $KClO_4$, $NaClO_4$, $NaNO_3$ and NaCl, respectively (Figs. 5(A) and (B)). As showed in Fig. 5(A), the foreign cations have negligible impact on the adsorption of Cu(II) to MGO. It shows no differences among the three different cations that may be due to the formation of inner-sphere surface complexes on MGO. The analogous result was shown in previous investigation [18]. Meanwhile, the influence of foreign anions was investigated and shown in Fig. 5(B). Likewise, the different anions have few effects on the adsorption percentages.

3.5. Influence of HA/FA

HA and FA are ubiquitous natural products, which can easily form complexes with various metal ions and have significant impact on the adsorption and transport of metal ions [41,47–49]. The effect of pH on Cu(II) sorption on MGO in the absence and presence of HA/FA is shown in Fig. 6(A). It is apparent that the presence of HA/FA has beneficial effect on Cu(II) removal at low pH and has suppressed impact at high pH. Generally, it had been considered that the HA and FA are negatively charged at pH > 2.0. Thus, at low pH values, with the role of electrostatic attraction, the negatively charged HA/FA can be easily and effectively adsorbed on the positively charged surfaces of MGO to get the HA/FA–MGO hybrids. The HA/FA–MGO hybrids can amend the long-term electrostatic capability of the solid–liquid interphase, which produces a more advantageous electrostatic circumstance for the Cu(II) sorption and promotes the construction of ternary surface complexes (HA/FA–MGO–Cu(II)). Moreover, the other vital factor for the improvement of Cu(II) removal in the presence of HA/FA is that the reduction happens on the sorption between MGO and HA/FA, which gives rise to more advantageous electrostatic forces with copper ions in solutions. However, the surfaces of MGO becomes negatively charged at high pH values, and it is difficult to absorb the negatively charged HA/FA because of the electrostatic repulsive forces. Meanwhile, the soluble HA/FA competes to MGO on the sorption of copper ions, which forms the stable HA/FA–Cu complexes in the solution and leads to the decline of Cu(II) removal by MGO [8]. In previous investigations, Sheng et al. [18,41] studied HA/FA effects on adsorption behavior of Cu(II) on raw and plasma-induced polyaniline-grafted MWCNTs, Zhang et al. [50] studied the effect of HA/FA on the Cu(II) removal by ZSM-5 zeolite. Li et al. [8] studied the influence of FA on the Cu(II) uptake mechanisms on GO/Fe_3O_4. Hu et al. [51] studied the removal of Cu(II) by β-cyclodextrin modified multiwall carbon nanotube/iron oxides in the absence/presence of FA, and similar foundlings have been reported.

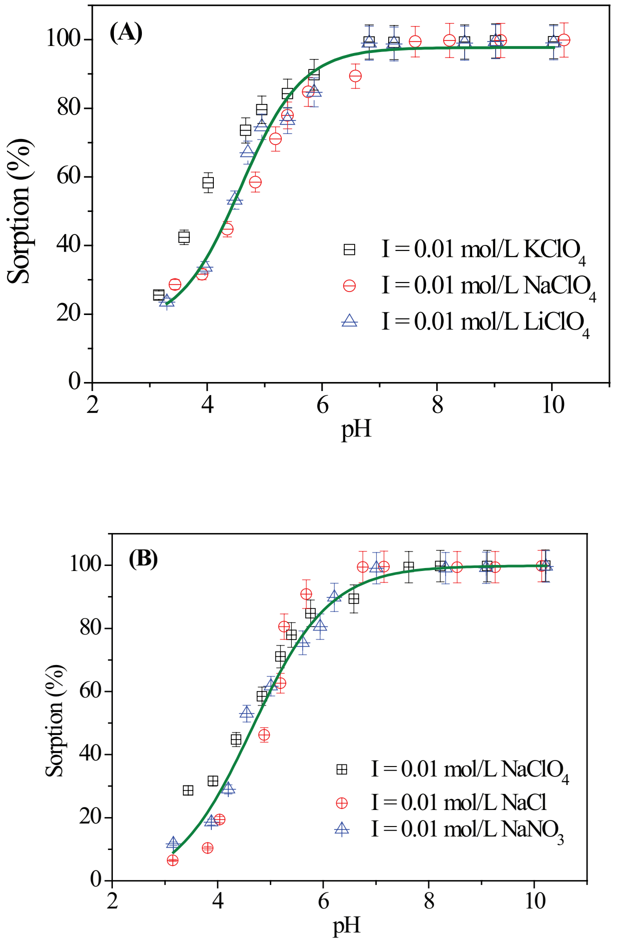

Fig. 5. Influence of (A) cations and (B) anions on Cu(II) adsorption onto MGO as a function of pH, $C_{Cu} = 15$ mg/L, $m/V = 0.1$ g/L, $T = 293$ K.

Meanwhile, the relationship of Cu(II) sorption percentages, C_e, and q_e in the absence and presence of HA/FA with various concentrations are expressed in 3D and shown in Figs. 6(B) and (C), respectively. From the shapes and trends, Figs. 6(B) and (C) are quite similar, which explains that HA and FA may play an equivalent role in the Cu(II) sorption onto GMO due to their same functional groups. From Figs. 6(B) and (C), the increase of HA/FA concentrations has an affirmative effect on Cu(II) removal. On the C_e–q_e plane, the sorption data were simulated by the Langmuir and Freundlich isotherm models, respectively (Figs. S1 and S2).

The Langmuir isotherm model can be described in the following form [52–56]:

$$q_e = \frac{bq_{\max}C_e}{1+bC_e} \tag{7}$$

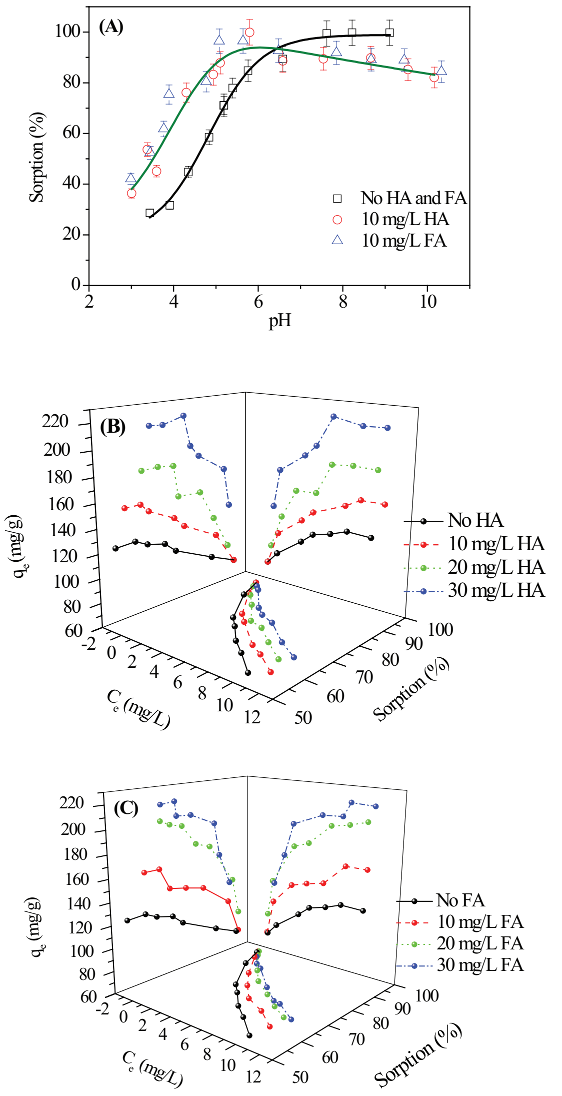

Fig. 6. (A) Influence of HA/FA on Cu(II) adsorption onto MGO as a function of pH, C_{Cu} = 15 mg/L, m/V = 0.1 g/L, I = 0.01 mol/L $NaClO_4$, T = 293 K. (B) 3D plots of q_e, C_e and sorption percentage in the presence of HA and (C) in the presence of FA, C_{Cu} = 15 mg/L, m/V = 0.1 g/L, I = 0.01 mol/L $NaClO_4$, T = 293 K.

And Eq. (6) can be transformed as the linear form:

$$\frac{C_e}{q_e} = \frac{C_e}{q_{\max}} + \frac{1}{bq_{\max}} \tag{8}$$

where b (L/g) and $q_{\max}$ (mg/g) are the Langmuir constants that is relevant to the adsorption energy and adsorption capacity, respectively.

The Freundlich isotherm model has the following equation [52–56]:

$$q_e = k_F C_e^{\,n} \tag{9}$$

Eq. (8) can also be converted to the linear form:

$$\log q_e = \log k_F + n \log C_e \tag{10}$$

where k_F ($mg^{1-n}L^n/g$) and n are the Freundlich parameters that represents the sorption capacity and the extant of dependence of adsorption, respectively. Table 2 shows the relative constants calculated from two models. From Table 2, it is clear that the correlation coefficients (R^2) of Langmuir and Freundlich model are ~1, indicating Langmuir and Freundlich model fit the sorption data well.

3.6. Thermodynamic study

The Cu(II) adsorption isotherms at T = 293, 313 and 333 K were studied and are shown in Fig. 7(A). In addition, the Langmuir and Freundlich simulation for the adsorption isotherms of Cu(II) on MGO are shown in Figs. 7(B) and (C), respectively. The parameters are listed in Table 1. The thermodynamic parameters ($\Delta H°$, $\Delta S°$ and $\Delta G°$) for Cu(II) adsorption onto GMO are calculated from the temperature-dependent adsorption. The $\Delta G°$ can be calculated from the following expression [8,36]:

$$\Delta G^0 = -RT \ln K^0 \tag{11}$$

where R = 8.314 J/(mol·K) is ideal gas constant, and K^0 is the parameter of adsorption equilibrium. The values of $\ln K^0$ are got by drawing $\ln K_d$–C_e context diagram and extrapolating C_e

Table 1
The parameters of Langmuir and Freundlich isotherm fitting of Cu(II) adsorption onto MGO

Conditions	Langmuir			Freundlich		
	$q_{\max}$ (mg/g)	b (L/g)	R^2	k_F (($mg^{1-n}L^n$)/g)	n	R^2
293 K, 10 mg/L HA	145.56	2.66	0.94	94.41	0.21	0.99
293 K, 20 mg/L HA	186.22	1.29	0.96	103.94	0.26	0.95
293 K, 30 mg/L HA	224.72	1.51	0.95	140.83	0.19	0.90
293 K, 10 mg/L FA	151.52	3.07	0.97	101.60	0.20	0.95
293 K, 20 mg/L FA	199.20	2.29	0.99	125.34	0.22	0.97
293 K, 30 mg/L FA	232.56	1.14	0.97	134.80	0.21	0.90
293 K, No HA/FA	127.23	1.78	0.99	85.11	0.16	0.97
313 K, No HA/FA	155.28	1.56	0.99	100.69	0.16	0.95
333 K, No HA/FA	185.87	2.16	0.99	124.45	0.17	0.97

Table 2
The values of $\ln K^0$ and thermodynamic parameters for the adsorption of Cu(II) on MGO at three different temperatures

T (K)	$\ln K^0$	$\Delta G°$ (kJ/mol)	$\Delta S°$ (J/(mol·K))	$\Delta H°$ (kJ/mol)
293	11.61	–28.28	132.5	10.54
313	12.06	–31.38	132.5	10.09
333	12.13	–33.58	132.5	10.54

to zero [57], and they are listed in Table 2. The values of standard entropy change ($\Delta S°$) are calculated from the equation:

$$\Delta S^0 = -\left(\frac{\partial \Delta G^0}{\partial T}\right)_p \tag{12}$$

The values of standard enthalpy change ($\Delta H°$) are obtained from the equation:

$$\Delta H° = \Delta G° + T\Delta S° \tag{13}$$

The values of thermodynamic parameters ($\Delta H°$, $\Delta S°$ and $\Delta G°$) are listed in Table 2, which provides a path to deduce the possible mechanism of Cu(II) sorption on MGO. It is definite that the Cu(II) adsorption process is endothermic because all the $\Delta H° > 0$. One possible reason for explaining this endothermic process is that copper ions is commendably solvated in the water, and the Cu(II) hydration shell must be decomposed before it is adsorbed by MGO. Much energy is needed during the dehydration process so that the higher temperature is more favorable for the sorption process [41]. It is supposed that the energies liberated during MGO adsorb copper ions are inferior to which the dehydration needed. The implicit hypothesis is that the adsorbed copper ions are more difficult to hydrate than those are in solution. Virtually, it is an endothermic reaction during the process about the removal of water from copper ions, and the endothermicity of the desolvation process transcends the enthalpy of adsorption to a considerable extent. The $\Delta G° < 0$ indicates that the Cu(II) sorption process is spontaneous. On the other hand, with the increasing of temperature, the $\Delta G°$ becomes more negative that indicates high temperature is more beneficial to Cu(II) adsorption. Because cations can be effortlessly desolvated at high temperature, their adsorption becomes more efficient. The $\Delta S° > 0$ implies that the confusion of the solid–solution system is increased, which may be caused by some structural changes in sorbate and adsorbent during the sorption process. From the thermodynamic analysis, it suggests that the Cu(II) adsorption by GMO is a spontaneous and endothermic process. As adsorption is an important technique in environmental pollution treatment [58–62], the MGO is a promising scavenger for the efficient sequestration of Cu(II) and related metals from wastewater.

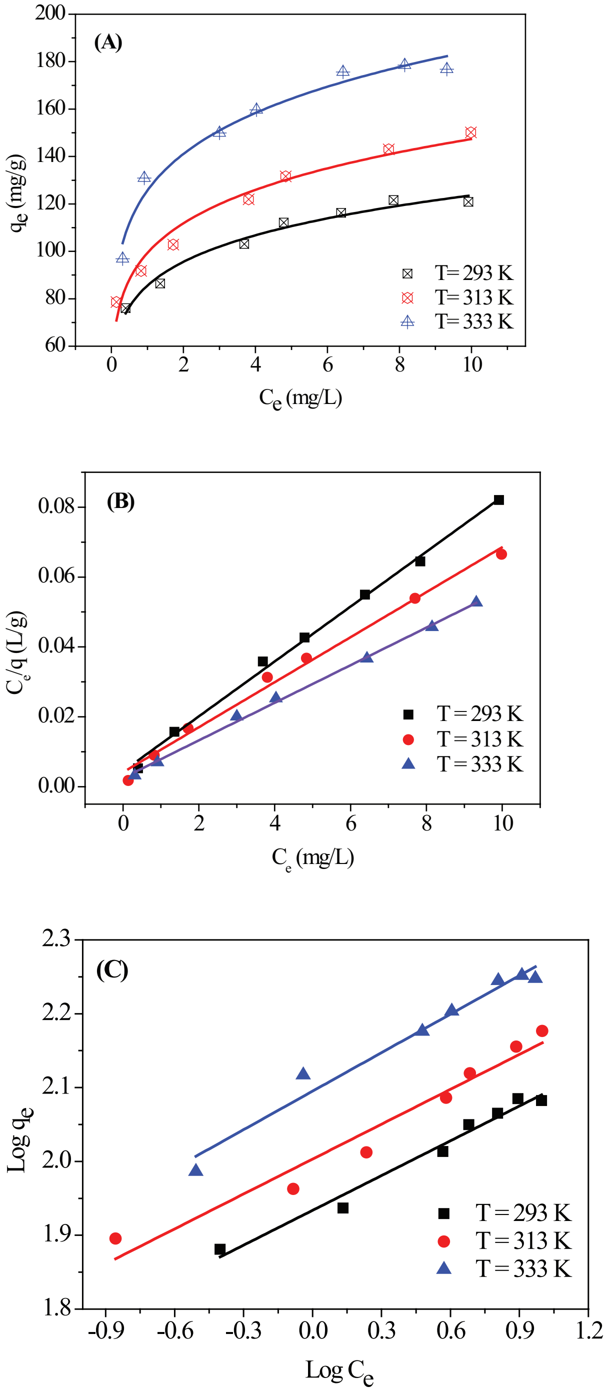

Fig. 7. (A) Adsorption isotherms of Cu(II) on MGO at three temperatures. (B) Langmuir and (C) Freundlich model, $m/V = 0.1$ g/L, $I = 0.01$ mol/L $NaClO_4$.

4. Conclusion

In summary, the MGO was synthesized and Cu(II) adsorption on MGO in the absence and presence of HA/FA was investigated by utilizing batch experiment (Fig. 8). From the experimental results, the conclusions are as follows: (1) Cu(II) sorption onto MGO is fast and can be well described by the pseudo-second-order model; (2) The capture of Cu(II) on MGO has strong dependence on pH but independence on ionic strength. The Cu(II) removal is mainly accomplished by inner-sphere complexation; (3) The presence of HA/FA is favorable for Cu(II) removal at low pH but is adverse at high pH; (4) The Langmuir and Freundlich model fit the adsorption isotherm as well; (5) The thermodynamic data confirm

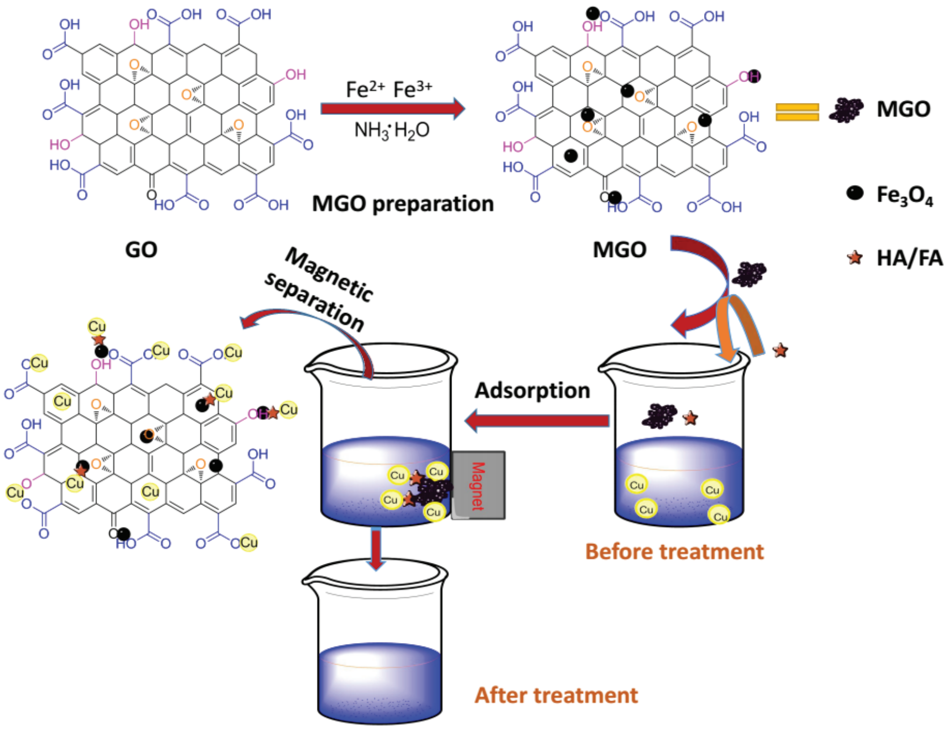

Fig. 8. Schematic illustration for the preparation process of MGO and its application in the removal of Cu(II) from aqueous solution.

that the sorption process is endothermic and spontaneous; and (6) The application of MGO in the treatment of copper ions can provide a new way for treating other heavy ions.

Acknowledgment

Financial supports from the National Natural Science Foundation of China (21577093, 21207092), Natural Science Foundation of Zhejiang Province (LY15B070001) is greatly acknowledged.

References

[1] P.A. Brown, S.A. Gill, S.J. Allen, Metal removal from waste water using peat, Water Res., 34 (2000) 3907–3916.

[2] D. Ozdes, A. Gundogdu, B. Kemer, C. Duran, H.B. Senturk, M. Soylak, Removal of Pb(II) ions from aqueous solution by a waste mud from copper mine industry: equilibrium, kinetic and thermodynamic study, J. Hazard. Mater., 166 (2009) 1480–1487.

[3] A.K. Mishra, S. Ramaprabhu, Magnetite decorated multiwalled carbon nanotube based supercapacitor for arsenic removal and desalination of seawater, J. Phys. Chem. C, 114 (2010) 2583–2590.

[4] M.R. Awual, M. Ismael, T. Yaita, S.A. El-Safty, H. Shiwaku, Y. Okamoto, S. Suzuki, Trace copper(II) ions detection and removal from water using novel ligand modified composite adsorbent, Chem. Eng. J., 222 (2013) 67–76.

[5] G.X. Yang, H. Jiang, Amino modification of biochar for enhanced adsorption of copper ions from synthetic wastewater, Water Res., 48 (2014) 396–405.

[6] M.R. Awual, T. Yaita, S.A. El-Safty, H. Shiwaku, S. Suzuki, Y. Okamoto, Copper(II) ions capturing from water using ligand modified a new type mesoporous adsorbent, Chem. Eng. J., 221 (2013) 322–330.

[7] Y.Y. Ge, X.M. Cui, Y. Kong, Z.L. Li, Y. He, Q.Q. Zhou, Porous geopolymeric spheres for removal of Cu(II) from aqueous solution: synthesis and evaluation, J. Hazard. Mater., 283 (2015) 244–251.

[8] J. Li, S.W. Zhang, C.L. Chen, G.X. Zhao, X. Yang, J.X. Li, K.X. Wang, Removal of Cu(II) and fulvic acid by graphene oxide nanosheets decorated with Fe_3O_4 nanoparticles, ACS Appl. Mater. Interfaces, 4 (2012) 4991–5000.

[9] X.N. Tang, Q. Zhang, Z.G. Liu, K.F. Pan, Y.H. Dong, Y.Y. Li, Removal of Cu(II) by loofah fibers as a natural and low-cost adsorbent from aqueous solutions, J. Mol. Liq., 199 (2014) 401–407.

[10] L. Zhang, Y.H. Zhao, R. Bai, Development of a multifunctional membrane for chromatic warning and enhanced adsorptive removal of heavy metal ions: application to cadmium, J. Membr. Sci., 379 (2011) 69–79.

[11] J. Matusik, A. Wścisło, Enhanced heavy metal adsorption on functionalized nanotubular halloysite interlayer grafted with aminoalcohols, Appl. Clay Sci., 100 (2014) 50–59.

[12] F.A. Abu Al-Rub, M.H. El-Naas, I. Ashour, M. Al-Marzouqi, Biosorption of copper on *Chlorella vulgaris* from single, binary and ternary metal aqueous solutions, Process Biochem., 41 (2006) 457–464.

[13] T.A. Kurniawan, G.Y.S. Chan, W.H. Lo, S. Babel, Physico–chemical treatment techniques for wastewater laden with heavy metals, Chem. Eng. J., 118 (2006) 83–98.

[14] Y.P. Kumar, P. King, V.S.R.K. Prasad, Equilibrium and kinetic studies for the biosorption system of copper(II) ion from aqueous solution using *Tectona grandis* L.f. leaves powder, J. Hazard. Mater., 137 (2006) 1211–1217.

[15] J.J. Wang, Z.K. Li, Enhanced selective removal of Cu(II) from aqueous solution by novel polyethylenimine-functionalized ion imprinted hydrogel: behaviors and mechanisms, J. Hazard. Mater., 300 (2015) 18–28.

[16] L. Curkovic, S. Cerjan-Stefanovic, A. Rastovean-Mioe, Batch Pb^{2+} and Cu^{2+} removal by electric furnace slag, Water Res., 35 (2001) 3436–3440.

[17] N. Chiron, R. Guilet, E. Deydier, Adsorption of Cu(II) and Pb(II) onto a grafted silica: isotherms and kinetic models, Water Res., 37 (2003) 3079–3086.

[18] G.D. Sheng, Y.M. Li, H.P. Dong, D.D. Shao, Environmental condition effects on radionuclide ^{64}Cu(II) sequestration to a novel composite: polyaniline grafted multiwalled carbon nanotubes, J. Radioanal. Nucl. Chem., 293 (2012) 797–806.

[19] M.H. Al-Qunaibit, W.K. Mekhemer, A.A. Zaghloul, The adsorption of Cu(II) ions on bentonite—a kinetic study, J. Colloid Interface Sci., 283 (2005) 316–321.

[20] H. He, J. Klinowski, M. Forster, A new structural model for graphite oxide, Chem. Phys. Lett., 287 (1998) 53–56.

[21] G. Zhao, J. Li, X. Ren, C. Chen, X. Wang, Few-layered graphene oxide nanosheets as superior sorbents for heavy metal ion pollution management, Environ. Sci. Technol., 45 (2011) 10454–10462.

[22] M. Liu, C. Chen, J. Hu, X. Wu, X.K. Wang, Synthesis of magnetite/graphene oxide composite and application for cobalt(II) removal, J. Phys. Chem. C, 115 (2011) 25234–25240.

[23] J. Zhu, S. Wei, H. Gu, S.B. Rapole, Q. Wang, Z. Luo, N. Haldolaarachchige, D.P. Young, Z. Guo, One-pot synthesis of magnetic graphene nanocomposites decorated with core@double-shell nanoparticles for fast chromium removal, Environ. Sci. Technol., 46 (2011) 977–985.

[24] Y. Yao, S. Liu, L.P. Ma, H. Sun, S. Wang, Synthesis, characterization, and adsorption properties of magnetic Fe_3O_4@graphene nanocomposite, Chem. Eng. J., 184 (2012) 326–332.

[25] C. Wang, C. Feng, Y.J. Gao, X.X. Ma, Q.H. Wu, Z. Wang, Preparation of a graphene-based magnetic nanocomposite for the removal of an organic dye from aqueous solution, Chem. Eng. J., 173 (2011) 92–97.

[26] G.D. Sheng, Y.M. Li, X. Yang, X.M. Ren, S.T. Yang, J. Hu, X.K. Wang, Efficient removal of arsenate by versatile magnetic graphene oxide composites, RSC Adv., 2 (2012) 12400–12407.

[27] L. Hao, H. Song, L. Zhang, X. Wan, Y. Tang, Y. Lv, SiO_2/graphene composite for highly selective adsorption of Pb(II) ion, J. Colloid Interface Sci., 369 (2012) 381–387.

[28] L.M. Cui, Y.G. Wang, L. Gao, L.H. Hu, L.G. Yan, Q. Wei, B. Du, EDTA functionalized magnetic graphene oxide for removal of Pb(II), Hg(II) and Cu(II) in water treatment: adsorption mechanism and separation property, Chem. Eng. J., 281 (2015) 1–10.

[29] B.C. Qiu, Q.Y. Li, B. Shen, M.Y. Xing, J.L. Zhang, Stöber-like method to synthesize ultradispersed Fe_3O_4 nanoparticles on graphene with excellent photo-Fenton reaction and high-performance lithium storage, Appl. Catal., B, 183 (2016) 216–223.

[30] S.L. Wan, F. He, J.Y. Wu, W.B. Wan, Y.W. Gu, B. Gao, Rapid and highly selective removal of lead from water using graphene oxide-hydrated manganese oxide nanocomposites, J. Hazard. Mater., 314 (2016) 32–40.

[31] V. Chandra, J. Park, Y. Chun, J.W. Lee, I.C. Hwang, K.S. Kim, Water-dispersible magnetite-reduced graphene oxide composites for arsenic removal, ACS Nano, 4 (2010) 3979–3986.

[32] F. Yu, S.N. Sun, J. Ma, S. Han, Enhanced removal performance of arsenate and arsenite by magnetic graphene oxide with high iron oxide loading, Phys. Chem. Chem. Phys., 17 (2015) 4388–4397.

[33] H. Wang, Y.G. Liu, G.M. Zeng, X.J. Hu, X. Hu, T.T. Li, H.Y. Li, Y.Q. Wang, L.H. Jiang, Grafting of β-cyclodextrin to magnetic graphene oxide via ethylenediamine and application for Cr(VI) removal, Carbohydr. Polym., 113 (2014) 166–173.

[34] J.W. Zhang, M.S. Azam, C. Shi, J. Huang, B. Yan, Q.X. Liu, H.B. Zeng, Poly(acrylic acid) functionalized magnetic graphene oxide nanocomposite for removal of methylene blue, RSC Adv., 5 (2015) 32272–32282.

[35] G.C. Chen, X.Q. Shan, Y.S. Wang, Z.G. Pei, X.E. Shen, B. Wen, G. Owens, Effects of copper, lead, and cadmium on the sorption and desorption of atrazine onto and from carbon nanotubes, Environ. Sci. Technol., 42 (2008) 8297–8302.

[36] S.T. Yang, G.D. Sheng, X.L. Tan, J. Hu, J.Z. Du, G. Montavon, X.K. Wang, Determination of Ni(II) uptake mechanisms on mordenite surfaces: a combined macroscopic and microscopic approach, Geochim. Cosmochim. Acta, 75 (2011) 6520–6534.

[37] W.S. Hummers Jr., R.E. Offeman, Preparation of graphitic oxide, J. Am. Chem. Soc., 80 (1958) 1339–1341.

[38] P. Bradder, S.K. Ling, S. Wang, S. Liu, Dye adsorption on layered graphite oxide, J. Chem. Eng. Data, 56 (2010) 138–141.

[39] Y.S. Ho, G. McKay, Pseudo-second order model for sorption processes, Process Biochem., 34 (1999) 451–465.

[40] G.X. Zhao, H.X. Zhang, Q.H. Fan, X.M. Ren, J.X. Li, Y.X. Chen, X.K. Wang, Sorption of copper(II) onto super-adsorbent of bentonite–polyacrylamide composites, J. Hazard. Mater., 173 (2010) 661–668.

[41] G.D. Sheng, J.X. Li, D.D. Shao, J. Hu, C.L. Chen, Y.X. Chen, X.K. Wang, Adsorption of copper(II) on multiwalled carbon nanotubes in the absence and presence of humic or fulvic acids, J. Hazard. Mater., 178 (2010) 333–340.

[42] Y.J. Lee, E.J. Elzinga, R.J. Reeder, Cu(II) adsorption at the calcite–water interface in the presence of natural organic matter: kinetic studies and molecular-scale characterization, Geochim. Cosmochim. Acta, 69 (2005) 49–61.

[43] S.T. Yang, G.D. Sheng, Z.Q. Guo, X.L. Tan, J.Z. Xu, X.K. Wang, Investigation of radionuclide ^{63}Ni(II) sequestration mechanisms on mordenite by batch and EXAFS spectroscopy study, Sci. China Chem., 55 (2012) 632–642.

[44] S.B. Yang, J. Hu, C.L. Chen, D.D. Shao, X.K. Wang, Mutual effects of Pb(II) and humic acid adsorption on multiwalled carbon nanotubes/polyacrylamide composites from aqueous solutions, Environ. Sci. Technol., 45 (2011) 3621–3627.

[45] K.F. Hayes, J.O. Leckie, Modeling ionic strength effects on cation adsorption at hydrous oxide/solution interfaces, J. Colloid Interface Sci., 115 (1987) 564–572.

[46] J.X. Li, J. Hu, G.D. Sheng, G.X. Zhao, Q. Huang, Effect of pH, ionic strength, foreign ions and temperature on the adsorption of Cu(II) from aqueous solution to GMZ bentonite, Colloids Surf., A, 349 (2009) 195–201.

[47] S. Ghosh, H. Mashayekhi, B. Pan, P. Bhowmik, B.S. Xing, Colloidal behavior of aluminum oxide nanoparticles as affected by pH and natural organic matter, Langmuir, 24 (2008) 12385–12391.

[48] S.F. Lim, Y.M. Zheng, S.W. Zou, J.P. Chen, Removal of copper by calcium alginate encapsulated magnetic sorbent, Chem. Eng. J., 152 (2009) 509–513.

[49] K. Yang, B. Xing, Adsorption of fulvic acid by carbon nanotubes from water, Environ. Pollut., 157 (2009) 1095–1100.

[50] L.P. Zhang, H. Zhang, X.J. Yu, Investigation of solution chemistry effects on sorption behavior of Cu(II) on ZSM-5 zeolite, Water Environ. Res., 83 (2011) 2170–2177.

[51] J. Hu, S.T. Yang, X.K. Wang, Adsorption of Cu(II) on β-cyclodextrin modified multiwall carbon nanotube/iron oxides in the absence/presence of fulvic acid, J. Chem. Technol. Biotechnol., 87(2012) 673–681.

[52] J. Li, Z.Y. Shao, C.L. Chen, X.K. Wang, Hierarchical GOs/Fe_3O_4/PANI magnetic composites as adsorbent for ionic dye pollution treatment, RSC Adv., 4 (2014) 38192–38198.

[53] Z.Q. Guo, Y. Li, S.W. Zhang, H.H. Niu, Z.S. Chen, J.Z. Xu, Enhanced sorption of radiocobalt from water by Bi(III) modified montmorillonite: a novel adsorbent, J. Hazard. Mater., 192 (2011) 168–175.

[54] X.L. Sun, X.G. Liu, B.J. Yang, L.C. Xu, S.M. Yu, Functionalized chrysotile nanotubes with mercapto groups and their Pb(II) and Cd(II) adsorption properties in aqueous solution, J. Mol. Liq., 208 (2015) 347–355.

[55] G.Z. Kyzas, Z. Terzopoulou, V. Nikolaidis, E. Alexopoulou, D.N. Bikiaris, Low-cost hemp biomaterials for nickel ions removal from aqueous solutions, J. Mol. Liq., 209 (2015) 209–218.

[56] Y. Zhang, L.Z. Bai, W.F. Zhou, R.H. Lu, H.X. Gao, S.B. Zhang, Superior adsorption capacity of Fe_3O_4@nSiO_2@mSiO_2 core-shell microspheres for removal of congo red from aqueous solution, J. Mol. Liq., 219 (2016) 88–94.

[57] P.P. Chang, X.K. Wang, S.M. Yu, W.S. Wu, Sorption of Ni(II) on Na-rectorite from aqueous solution: effect of pH, ionic strength and temperature, Colloids Surf., A, 302 (2007) 75–81.

[58] S.J. Yu, X.X. Wang, Y.J. Ai, Y. Liang, Y.F. Ji, J.X. Li, T. Hayat, A. Alsaedi, X.K. Wang, Spectroscopic and theoretical studies on the counterion effect of Cu(II) ion and graphene oxide interaction with titanium dioxide, Environ. Sci. Nano, 3 (2016) 1361–1368.

[59] Y.D. Zou, X.X. Wang, Z.S. Chen, W. Yao, Y.J. Ai, Y.H. Liu, T. Hayat, A. Alsaedi, N.S. Alharbi, X.K. Wang, Superior coagulation of graphene oxides on nanoscale layered double hydroxides and layered double oxides, Environ. Pollut., 219 (2016) 107–117.

[60] X.X. Wang, S.J. Yu, J. Jin, H.Q. Wang, N.S. Alharbi, A. Alsaedi, T. Hayat, X.K. Wang, Application of graphene oxides and graphene oxide-based nanomaterials in radionuclide removal from aqueous solutions, Sci. Bull., 61 (2016) 1583–1593.

[61] S.J. Yu, X.X. Wang, S.T. Yang, G.D. Sheng, A. Alsaedi, T. Hayat, X.K. Wang, Interaction of radionuclides with natural and manmade materials using XAFS technique, Sci. China Chem., 60 (2017) 170–187.

[62] Y.B. Sun, X.X. Wang, W.C. Song, S.H. Lu, C.L. Chen, X.K. Wang, Mechanistic insights on the decontamination of Th(IV) on graphene oxide-based composites by EXAFS and modeling techniques, Environ. Sci. Nano, 4 (2017) 222–232.

Supplementary material

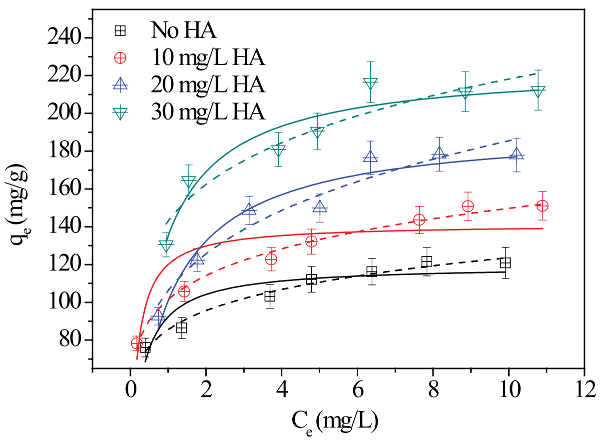

Fig. S1. Langmuir and Freundlich non-linear plots of adsorption isotherms for Cu(II) onto MGO in the absence and presence of HA. The solid lines are Langmuir model simulation, and the dashed lines are Freundlich model simulation, C_{Cu} = 15 mg/L, m/V = 0.1 g/L, I = 0.01 mol/L $NaClO_4$, T = 293 K.

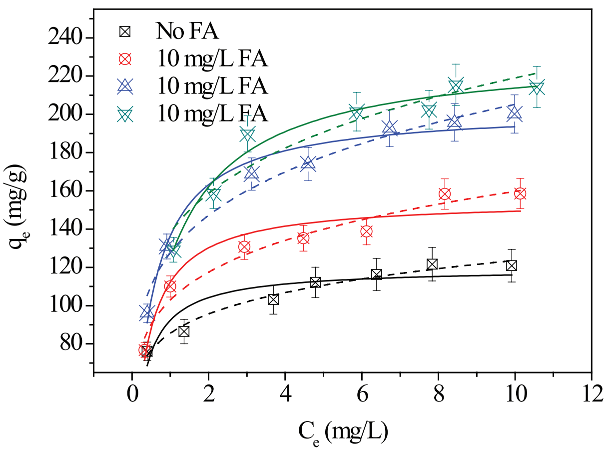

Fig. S2. Langmuir and Freundlich non-linear plots of adsorption isotherms for Cu(II) onto MGO in the absence and presence of FA. The solid lines are Langmuir model simulation, and the dashed lines are Freundlich model simulation, C_{Cu} = 15 mg/L, m/V = 0.1 g/L, I = 0.01 mol/L $NaClO_4$, T = 293 K.